NEOPLASIA
www.neoplasia.com

Volume 20 Number 2 February 2018 pp. 119–130 119

A Low-Toxicity DNA-Alkylating *N*-Mustard-Quinoline Conjugate with Preferential Sequence Specificity Exerts Potent Antitumor Activity Against Colorectal Cancer

Tai-Lin Chen[*,†,‡], Yi-Wen Lin[‡], Yan-Bo Chen[†], Jing-Jer Lin[§], Tsann-Long Su[‡], Chia-Ning Shen [†] and Te-Chang Lee[‡,¶]

*Institute of Biochemistry and Molecular Biology, National Yang-Ming University, Taipei 11221, Taiwan; [†]Genomics Research Center, Academia Sinica, Taipei 11529, Taiwan; [‡]Institute of Biomedical Sciences, Academia Sinica, Taipei 11529, Taiwan; [§]Institute of Biochemistry and Molecular Biology, National Taiwan University College of Medicine, Taipei 10051, Taiwan; [¶]Institute of Pharmacology, National Yang-Ming University, Taipei 11221, Taiwan

Abstract

Efficacy and safety are fundamental prerequisites for anticancer drug development. In the present study, we explored the anti–colorectal cancer (CRC) activity of SL-1, a DNA-directed *N*-mustard-quinoline conjugate. The *N*-mustard moiety in SL-1 induced DNA strand breaks, interstrand cross-links (ICLs), G2/M arrest, and apoptosis, whereas its quinoline moiety preferentially directed SL-1 to target the selective guanine sequence 5′-G-G/C-N-G-C/T-3′. Notably, SL-1 was highly cytotoxic to various CRC cell lines. Experiments using xenograft models revealed that SL-1 was more potent than 5-fluorouracil (5-FU) and oxaliplatin for suppressing the growth of RKO and RKO-E6 (oxaliplatin-resistant subline) cells as well as metastatic SW620 cells. In addition, SL-1 combined with 5-FU was more effective than oxaliplatin and 5-FU for suppressing RKO or SW620 cell growth in mice. Significantly, compared with cisplatin, oxaliplatin, or 5-FU, SL-1 alone or in combination with 5-FU did not cause obvious kidney or liver toxicity in ICR mice. In summary, SL-1, a DNA-directed alkylating agent, is established as an anti-CRC agent with high efficacy and low toxicity and thus warrants further development for the treatment of CRC patients.

Neoplasia (2018) 20, 119–130

Introduction

DNA-alkylating agents were the first chemotherapeutic drugs developed for the treatment of cancer [1]. Although the classic, highly reactive DNA-alkylating agents (e.g., melphalan, chlorambucil, and platinum-based agents) are potent chemotherapeutic agents, they have limited clinical benefits mainly because of their toxicity, which results in severe adverse side effects [2]. The toxicity associated with DNA-alkylating agents highlights the need to develop anticancer agents with greater selectivity. To overcome the drawbacks of alkylating agents, which lack intrinsic DNA-binding affinity and thus are genotoxic and carcinogenic [3], DNA-directed alkylating agents with increased DNA-binding selectivity were designed to avoid "off-target" effects on cellular components and hence reduce adverse side effects [4]. Accordingly, we and many other scientists have previously synthesized a series of DNA-directed alkylating agents by coupling various DNA-affinic carriers (a DNA-intercalating agent or a DNA minor groove binder) that directly target DNA with the *N*-mustard pharmacophore [5–10]. These DNA-directed alkylating agents were shown to have increased chemical stability and improved anticancer activity.

Based on structural-activity relationship studies, selecting the appropriate DNA-affinic carrier and the spacer, which links to the

Abbreviations: AST, aspartate transaminase; ALT, alanine transaminase; BUN, blood urea nitrogen; CBC, complete blood count; CRC, colorectal cancer; DMSO, dimethyl sulfoxide; D5W, 5% dextrose isotonic solution; FHC, fetal human colon epithelial cells; H&E, hematoxylin and eosin; ICL, interstrand crosslink; i.p., intraperitoneal; i.v., intravenous; mCRC, metastatic CRC; PBS, Phosphate-buffered saline; PI, propidium iodide; p53-MT, p53 mutant; p53-WT, p53 wild-type; 5-FU, 5-fluorouracil

Address all correspondence to: Te-Chang Lee, Institute of Biomedical Sciences, Academia Sinica, Nankang, Taipei 11529, Taiwan. E-mail: bmtcl@ibms.sinica.edu.tw or Chia-Ning Shen, Genomics Research Center, Academia Sinica, Nankang, Taipei 11529, Taiwan. E-mail: cnshen@gate.sinica.edu.tw

Received 4 September 2017; Revised 9 November 2017; Accepted 13 November 2017

1476-5586
https://doi.org/10.1016/j.neo.2017.11.006

alkylating warhead, is critical for improving the antitumor activity of DNA-directed alkylating agents [11,12] In 1991, Denny and coworkers first synthesized *N*-mustard-quinoline conjugates that exerted potent cytotoxicity by forming DNA cross-links and bulky monoadducts [4]. Additionally, *N*-mustard-quinoline derivatives were found to overcome the poor solubility and low DNA-binding selectivity of some DNA intercalators, such as acridine mustard conjugates [9]. To improve the antitumor activity and increase the chemical stability of DNA-affinic *N*-mustards, we previously designed and synthesized a series of conjugates by coupling the *N*-mustard residue to quinoline moieties *via* a urea or hydrazine-carboxamide linker [13]. We found that these *N*-mustard-quinoline conjugates were chemically stable in serum and possessed strong growth inhibitory activity against human lymphoblastic leukemia and a panel of solid tumor cell lines [13]. These compounds also displayed limited systemic toxicity in animals. Among them, we noted that compound 18c, redesignated SL-1 (Figure 1*A*), was the most potent suppressor of the growth of breast carcinoma MX-1 xenografts, even achieving complete tumor remission [13]. These results indicate that SL-1 is a potential lead and warrants further investigation.

During the past three decades, platinum-based DNA-alkylating agents have been employed in the treatment of various cancers [14]. Oxaliplatin is currently used as a first-line treatment for colorectal cancer (CRC) [15]. Unfortunately, a large portion of CRC patients receiving oxaliplatin-based chemotherapy develop chemoresistance and metastatic cancer in a short period of time [16,17]. In general,

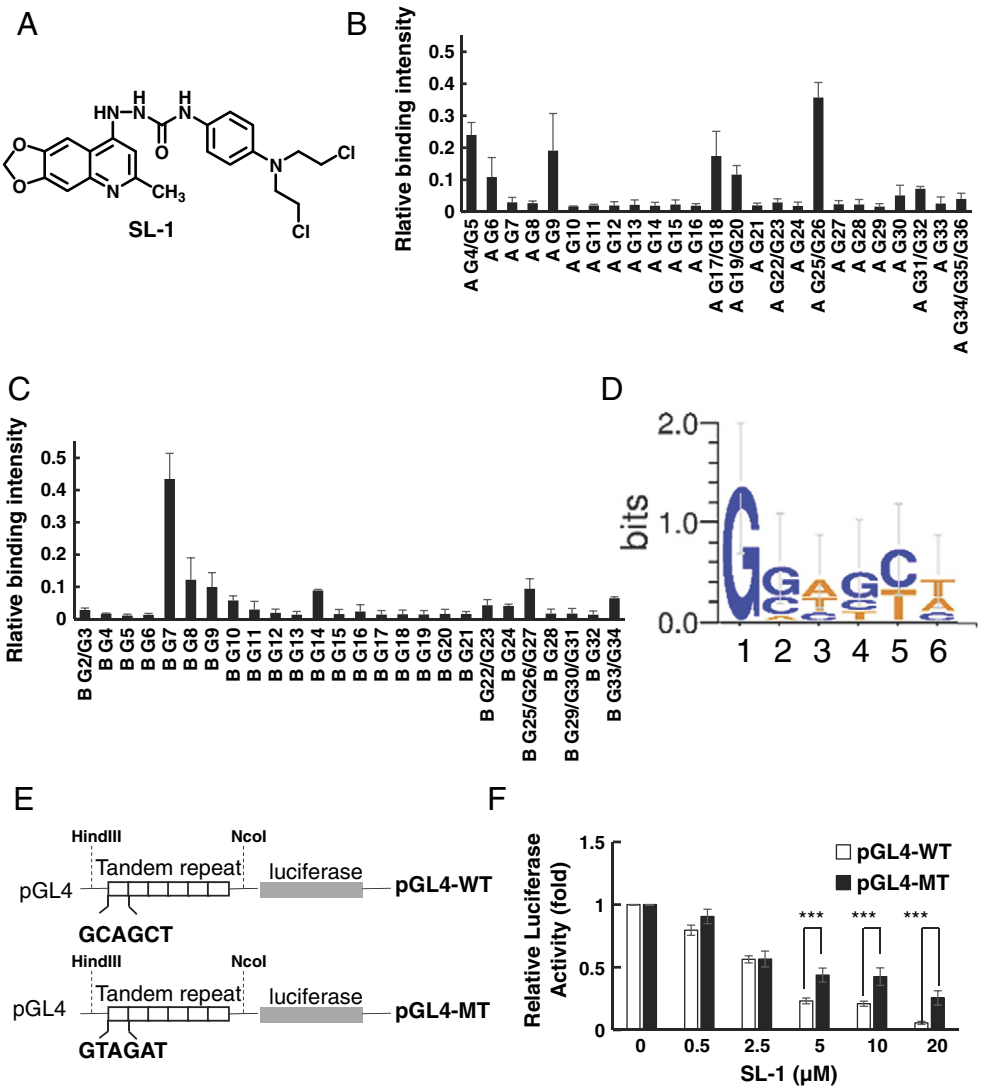

Figure 1. Interaction of SL-1 with specific DNA sequence. (A) Chemical structure of SL-1. (B, C) Differential N-7 guanine alkylation by SL-1 on the HexA-rev and HexB-rev fragments, respectively. As described in Materials and Methods, the relative binding intensities of individual guanines of HexA-rev and HexB-rev fragments were normalized by the Poisson distribution equation and plotted in (B) and (C), respectively. (D) Consensus sequence logo generated based on the weight using Seq2Logo Server 3.4. (E) Luciferase reporters with consensus or negative control segment. The reporters pGL4-WT and pGL4-MT were constructed by inserting six tandem repeats of consensus segment (5′-GCAGCT-3′) and the negative control (5′-GTAGAT-3′) into the luciferase pGL4-plasmid, respectively. (F) Significant inhibition of the luciferase reporter activity containing six tandem repeats of consensus segment (pGL4-WT) in RKO cells. RKO cells were transfected with *firefly* luciferase reporter (pGL4-WT or pGL4-MT) and *renilla* luciferase control reporter for 1 day and then treated with various concentrations of SL-1. The *firefly* luciferase reporter activity is presented as fold changes normalized to *renilla* luciferase activity and expressed as the means ± SD ($n = 3$). ***, $P < .001$, Student's *t* test.

metastatic CRC (mCRC) patients were treated with the combination regimen FOLFOX, including oxaliplatin, 5-fluorouracil (5-FU), and leucovorin, which improved response rates to >50%; however, because of its undesirable grade 3 to 4 toxicity, this regimen has a highly negative impact on quality of life [18,19]. Recently, standard chemotherapeutics have been used in combination with targeted therapeutic agents to ameliorate the mortality of patients with advanced CRC. However, the 5-year survival rate of patients with mCRC is still only 13% [19]. Therefore, the development of a novel treatment strategy for advanced CRC is required to fulfill this unmet need.

Discovering a novel agent that maintains therapeutic efficacy and reduces undesirable side effects is a fundamental requisite. Notably, among a series of DNA-directed alkylating agents, SL-1 was the most cytotoxic to CRC cells and showed limited toxicity to the animal [13]. Therefore, we sought to investigate the clinical potential of SL-1 as a therapeutic agent against CRC cells. However, the preferential sequence targeted by the quinoline moiety of SL-1 is unclear. In this study, we determined the sequence to which SL-1 preferentially binds, evaluated its anti-CRC activity, and determined its animal safety/toxicity. We also explored the efficacy and safety of the combination of SL-1 with 5-FU against CRC cells.

Materials and Methods

Chemicals and enzymes, chemical synthesis of SL-1, and cell culture are included in Supplementary Materials and Methods. The characteristics of the human CRC cell lines used in this study are summarized in Supplementary Table S1.

Drug-DNA Interactions

Sixty-four symmetrical hexanucleotide fragments (HexA-rev and HexB-rev fragments) [20,21] were labeled at the 3′-end and purified using polyacrylamide gel electrophoresis. The targeting of SL-1 to the guanine-N7 site was analyzed using the Maxam-Gilbert method [20–23] and confirmed by the luciferase reporter assay. Details are described in Supplementary Materials and Methods.

Functional Assays

In this study, the assays of cytotoxicity, alkaline agarose gel shift, comet and modified comet, flow cytometry, and annexin V staining were performed according to protocols as previously described [24,25]. Details are provided in Supplementary Materials and Methods.

Animal Studies

Animal studies including anticancer activity in xenograft mouse models and the toxicology examination in ICR mice are described in Supplementary Materials and Methods [24].

Results

SL-1 Specifically Targets the Pentameric Element 5′-G-G/C-N-G-C/T-3′

SL-1 was synthesized as previously described [13]. The chemical characteristics of SL-1 were confirmed by HRMS and NMR (Supplementary Figure S1, *A* and *B*) are summarized in Supplementary Table S2. The purity was >98% (Supplementary Figure S1*C*). Although SL-1 was designed as a DNA-directed alkylating agent, its targeted preferential sequence is unclear. The quinoline pharmacophore of SL-1 likely steers the compound to the DNA groove, whereas the *N*-mustard moiety contributes to alkylation anchoring to the N7-guanine residues. Using HexA-rev and HexB-rev fragments (Supplementary Figure S2*A*) as targets, we analyzed the SL-1–alkylated guanine adducts by the Maxam-Gilbert method. As shown in Supplementary Figure S2*B* and S1*C*, SL-1 predominantly bound to certain guanine residues, such as 5′-GG-3′ in HexA-rev and 5′-GC-3′ in HexB-rev. The relative binding intensities of SL-1 to individual guanine residues in HexA-rev and HexB-rev are plotted in Figure 1, *B* and *C*. Because SL-1 produced major adducts that, based on the molecular size of SL-1, covered at least five to six base pairs, the neighboring sequences of the guanine residue likely play certain roles in modulating the binding selectivity of SL-1. To analyze the consensus sequence for specific guanine adducts, the consensus logo was contributed by the sequences ranked in the top 50% of the relative binding intensities [26]. As shown in Figure 1*D*, the consensus sequence for SL-1 was 5′-G-G/C-N-G-C/T-3′ (N = any base). In addition, we found that the binding of SL-1 was abolished when a contiguous C was located at the 5′ end of G (5′-CG-3′). A similar binding pattern was observed using another *N*-mustard-quinoline conjugate called SL-2 (Supplementary Figure S3, *A* and B). The chemical characteristics of SL-2 are shown in Supplementary Figure S1 and Table S2).

To confirm the specific binding sequence of SL-1, a reporter assay with wild-type or mutant tandem repeats in front of the luciferase gene was constructed and evaluated for the preferential binding sequence of SL-1. As shown in Figure 1*E*, six repeats of the highly preferential sequence (5′-GCAGCT-3′) and mutant sequence (5′-GTAGAT-3′) were inserted into the pGL4 luciferase vector to form wild-type (pGL4-WT) and mutant (pGL4-MT) reporters, respectively. The pGL4-WT and pGL4-MT reporter plasmids were transfected into RKO cells and then treated with SL-1. As shown in Figure 1*F*, SL-1 inhibited the reporter activity of pGL4-WT more effectively than that of pGL4-MT, confirming that SL-1 preferentially interacted with 5-GCAGCT-3′ compared with 5′-GTAGAT-3′.

SL-1 Is Highly Cytotoxic to CRC Cell Lines

To assess whether SL-1 can be used as a therapeutic agent for CRC, we determined the cytotoxicity of SL-1 to a panel of CRC cell lines. As summarized in Table 1, SL-1 showed better cytotoxic effects than 5-FU, oxaliplatin, cisplatin, and irinotecan in a batch of p53 wild-type (p53-WT, i.e., HCT-116, RKO, LS174T, and LoVo cells) and mutant (p53-MT, i.e., RKO-E6, DLD-1, HT-29, SW620, and Caco-2 cells) CRC cell lines. The IC_{50} values of SL-1 in CRC cell lines ranged from 0.14 μM to 5.49 μM, which were 13- to 510-fold lower than that in normal colorectal epithelial cells (fetal human colon epithelial cells, FHC). By contrast, in comparison to the commonly used therapeutic agents 5-FU, oxaliplatin, cisplatin, and irinotecan, SL-1 was at least three-fold less cytotoxic to normal colonic epithelial FHC cells, indicating that SL-1 had a wider therapeutic window than these therapeutic agents.

To determine the cytotoxic mechanism of SL-1 in CRC cells, we performed alkaline gel electrophoresis, which demonstrated that treatment with SL-1 at concentrations as low as 0.05 μM induced moderate levels of ICLs (Figure 2*A*). However, upon further increasing the concentrations of SL-1, we observed a DNA smear, suggesting that SL-1 induced alkali-labile DNA alkylation. We also conducted comet and modified comet assays to determine the capability of SL-1 to cause DNA strand breaks and ICLs in cells. After incubating RKO cells with SL-1 for 48 hours, SL-1 induced an

Table 1. IC_{50} Values (Mean ± SD, μM) of SL-1, 5-FU, Irinotecan, Cisplatin, and Oxaliplatin in Human CRC cell Lines[a]

		p53-WT					p53-MT				p53-KO	
(μM)	FHC[b]	HCT116	RKO	LS174T	LoVo	Colo205	DLD-1	HT-29	SW620	Caco-2	RKO-E6[c]	H3347[d]
SL-1	71.47 ± 8.36 (1.0)[e]	0.34 ± 0.06 (210.2)	0.20 ± 0.08 (357.3)	4.55 ± 1.01 (15.7)	0.61 ± 0.03 (117.1)	0.46 ± 0.10 (155.3)	0.36 ± 0.07 (198.5)	0.53 ± 0.11 (134.8)	0.14 ± 0.06 (510.5)	5.49 ± 3.07 (13.0)	0.27 ± 0.06 (264.7)	0.23 ± 0.03 (310.7)
Oxaliplatin	19.69 ± 2.21 (1.0)	1.78 ± 0.11 (217.81)	0.62 ± 0.02 (625.3)	>50 (<0.39)	1.65 ± 0.21 (234.9)	2.26 ± 0.78 (171.5)	1.62 ± 0.06 (239.3)	1.92 ± 0.81 (201.9)	7.62 ± 3.12 (50.8)	1.64 ± 0.60 (236.4)	10.29 ± 3.39 (37.6)	2.55 ± 0.73 (152.0)
5-FU	21.90 ± 2.49 (1.0)	2.88 ± 0.33 (7.6)	6.15 ± 1.63 (3.5)	18.56 ± 0.26 (1.18)	25.81 ± 0.74 (0.8)	6.80 ± 3.05 (3.2)	16.89 ± 5.30 (1.3)	2.27 ± 0.41 (9.6)	18.5 ± 4.05 (1.1)	>50 (<0.4)	9.73 ± 4.53 (2.2)	5.89 ± 0.50 (3.7)
Cisplatin	21.04 ± 2.03 (1.0)	3.42 ± 0.36 (6.1)	26.3 ± 3.28 (0.8)	8.48 ± 2.74 (2.4)	6.38 ± 2.18 (3.3)	11.09 ± 1.27 (1.9)	29.63 ± 6.42 (0.7)	5.99 ± 1.22 (3.5)	0.91 ± 0.27 (23.1)	15.17 ± 5.19 (1.3)	24.83 ± 7.71 (0.8)	12.2 ± 0.64 (1.7)
Irinotecan	>100 (1.0)	1.38 ± 0.49 (>72.4)	2.63 ± 1.05 (>38.0)	1.36 ± 0.33 (>73.5)	9.69 ± 1.68 (>10.3)	2.49 ± 0.48 (>40.1)	1.72 ± 0.35 (>58.1)	4.19 ± 0.29 (>23.8)	0.32 ± 0.10 (>312.5)	21.28 ± 7.34 (>4.7)	2.70 ± 0.69 (>37.0)	2.93 ± 0.68 (>341.3)

[a] Data are the mean ± SD of three independent experiments.
[b] The FHC cell line was established from *normal human* fetal colonic mucosa.
[c] RKO-E6 cells contain a stably integrated human papilloma virus *E6* oncogene under control of the cytomegalovirus promoter and hence lack appreciably functional p53.
[d] H3347 is a human colon carcinoma *cell* line, but its molecular marker is not classified.
[e] Parentheses indicate the therapeutic index (IC_{50} FHC/IC_{50} tumor cell line).

increase in the tail moment in a dose-dependent manner (Figure 2*B* and Supplementary Figure S4*A*), suggesting that SL-1 caused DNA strand breaks or alkali-labile DNA damage in RKO cells. Moreover, similar to cisplatin, SL-1 treatment significantly induced DNA ICLs in RKO cells, as determined using the modified comet assay (Figure 2*C* and Supplementary Figure S4*B*). The doses required for SL-1 to induce DNA strand breaks or ICLs were at least 10-fold lower than those of cisplatin. In addition, SL-1 treatment resulted in a profound S phase delay at 24 hours and subsequent G2/M arrest at 48 and 72 hours in RKO cells in a dose-dependent manner (Figure 2*D*). We also observed a significant proportion of the SL-1–treated RKO cells entering into sub-G1 phase, suggesting that SL-1 treatment induced DNA damage that may trigger cell death. Overall, we demonstrated that SL-1 was a potent DNA damaging agent against CRC cells.

SL-1 Is a Potent Agent Against CRC Cells

To further explore the anticancer activity of SL-1 *in vivo*, we conducted animal studies by grafting RKO cells and their oxaliplatin-resistant subline, RKO-E6 cells, to athymic nude mice. Compared with oxaliplatin (Eloxatin, 7.5 mg/kg) and 5-FU (50 mg/kg), SL-1 (30 mg/kg) was the most potent suppressor of the growth of RKO tumor xenografts in nude mice (Figure 3*A*). On day 29, SL-1 suppressed tumor growth by approximately 65% compared with the positive control group. Notably, compared with oxaliplatin and 5-FU, SL-1 treatment also significantly inhibited tumor growth in mice engrafted with oxaliplatin-resistant RKO-E6 cells (Figure 3*B*). These results indicated that SL-1 was a potent anticancer agent against CRC.

The Combination of SL-1 and 5-FU Synergistically Suppresses Cell Growth

In clinical practice, various DNA targeting agents, such as oxaliplatin and irinotecan, are often used in combination with 5-FU to treat patients with CRC [27]. Therefore, we explored the efficacy of the combination of SL-1 with 5-FU for the treatment of RKO cells (a p53-WT cell line) and SW620 cells (a p53-MT cell line). As shown in Figure 4, a significant synergism was observed when RKO or SW620 cells were treated with SL-1 + 5-FU. The optimal ratio of SL-1 to 5-FU was apparently dependent on the cell type: 1:2 and 6:1 were optimal for RKO cells and SW620 cells, respectively. We further demonstrated that the combined treatment of RKO cells with SL-1 + 5-FU initially resulted in an accumulation of cells in S phase and then cell cycle arrest in G2/M phase (Figure 5*A*). Furthermore, the annexin V staining assay showed that 5-FU mainly caused necrotic cell death, whereas SL-1 primarily triggered apoptosis (Figure 5*B*). After a 72-hour treatment with the combination of SL-1 (0.75 μM) and 5-FU (1.5 μM), more than 80% of the observed cells were apoptotic.

Because the thymidylate synthase inhibitor 5-FU incorporates into RNA and DNA to induce DNA damage and trigger cell death [28], we performed a comet assay to evaluate the synergistic effect of SL-1 + 5-FU on DNA damage induction. As shown in Figure 5*C*, treatment of RKO cells with SL-1 + 5-FU for 24 hours synergistically extended the tail moment (34.6 ± 4.2 μm) compared with cells treated with SL-1 (5.4 ± 0.8 μm) or 5-FU (3.9 ± 0.4 μm) alone. Taken together, these results indicated that SL-1 + 5-FU had a synergistic effect on the induction of cytotoxicity and DNA damage in CRC cells.

Combined Treatment with SL-1 and 5-FU Significantly Suppresses Tumor Growth in Mice

Since SL-1 + 5-FU synergistically inhibited the growth of RKO and SW620 cells in culture, we further evaluated the effect of this combined treatment on the growth of CRC cells *in vivo*. Using RKO and SW620 xenograft models, we compared the effect of SL-1 + 5-FU to that of oxaliplatin + 5-FU. As shown in Figure 6*A*, SL-1 treatment at a dose of 30 mg/kg (Q2D×7, i.v. injection) significantly suppressed tumor growth of RKO xenografts by 61.8%, indicating that SL-1 treatment was more effective than the treatment with either oxaliplatin or 5-FU alone. Importantly, the efficacy of SL-1 + 5-FU (77.5% tumor suppression) was superior to that of oxaliplatin + 5-FU (47.5% tumor suppression). Furthermore, the mice treated with SL-1 + 5-FU exhibited no significant loss of body weight (Figure 6*A*). Based on cleaved caspase 3 and TUNEL immunostaining (Figure 6*B*), we further confirmed that increased apoptosis was observed in tumor tissues of mice treated with SL-1 + 5-FU. Similar growth suppression was observed in SW620-bearing mice treated with SL-1 + 5-FU (Figure 6*C*). However, in mice implanted with aggressive SW620 cells, the combined treatment with SL-1 + 5-FU caused only 10% body weight loss during the treatment period, and the body weight recovered after ending the treatment (Figure 6*C*). By contrast, the combined treatment with oxaliplatin + 5-FU resulted in approximately 20% body weight loss, suggesting that the combined

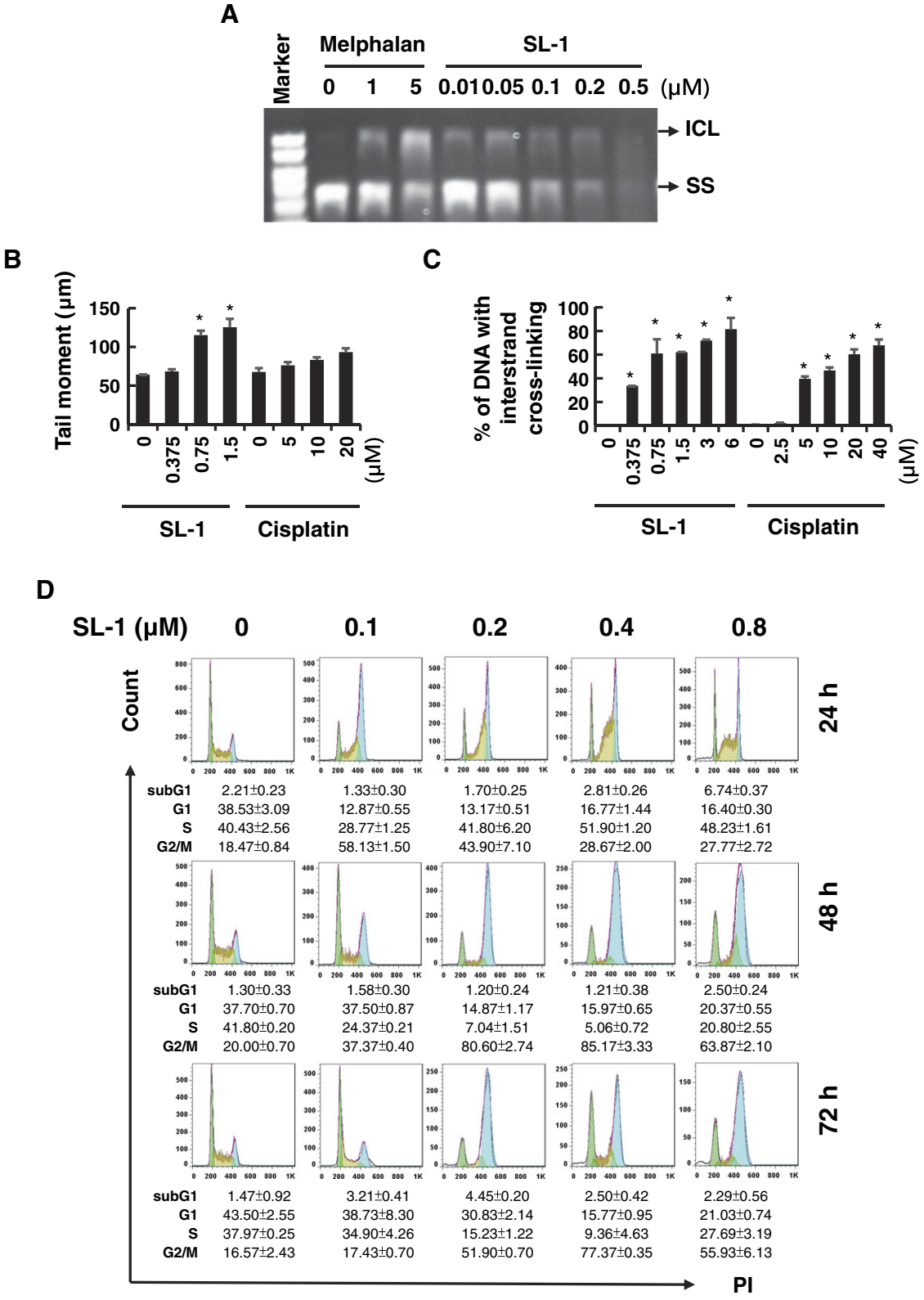

Figure 2. Induction of DNA damage and interference with cell cycle progression by SL-1. (A) Induced DNA ICLs by SL-1. The DNA plasmid pEGFP-N1 was incubated with SL-1 and subjected to alkaline agarose gel electrophoresis. *ICL*, interstrand crosslink; *SS*, single strand. (B) Induced DNA strand breaks in RKO cells by SL-1. RKO cells were treated with various concentrations of SL-1 or cisplatin as indicated for 48 hours. DNA strand breaks were evaluated by the comet assay. The data are the average of the median values of the tail moment (100 cells). Bar, SD of three independent experiments. (C) Induced DNA ICLs in RKO cells by SL-1. RKO cells were treated with various concentration of SL-1 or cisplatin as indicated for 2 hours. At the end of treatment, the cells were subjected to a modified comet assay. The percentages of DNA with ICLs were calculated as described in Material and Methods. The data represent the mean ± SD of three independent experiments. *, $P < .005$; Student's *t* test. (D) Interference with cell cycle progression by SL-1. RKO cells were treated with various doses of SL-1 for 24, 48, and 72 hours. Cell cycle analysis was performed using flow cytometry as described in Materials and Methods.

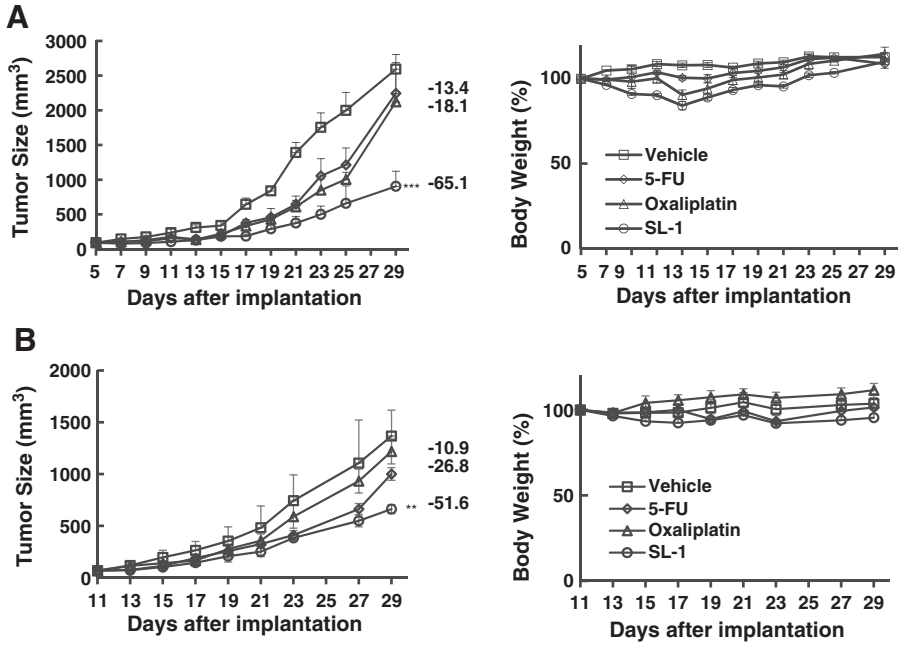

Figure 3. Inhibition of xenograft growth of RKO (p53-WT) and RKO-E6 (p53-KO) by SL-1. (A) RKO (5×10^6) and (B) RKO-E6 (5×10^6) cells were subcutaneously implanted into nude mice ($N = 4$-5). When the tumor size reached approximately 75-100 mm^3, the mice were randomly divided into four groups and treated with the following regimens: vehicle (DMSO/Tween 80/D5W = 1:1:8, i.v. every other days 7 times), SL-1 (30 mg/kg in the vehicle, i.v. every other days 7 times), oxaliplatin (Eloxatin®, 7.5 mg/kg in D5W, i.v. once a week 2 times), or 5-FU (50 mg/kg in D5W, i.p. once a week 2 times). The tumor volume (left) and body weight change (right) of the mice were recorded. The values presented are the mean ± SD of each group. ***, $P < .01$; Student's *t* test.

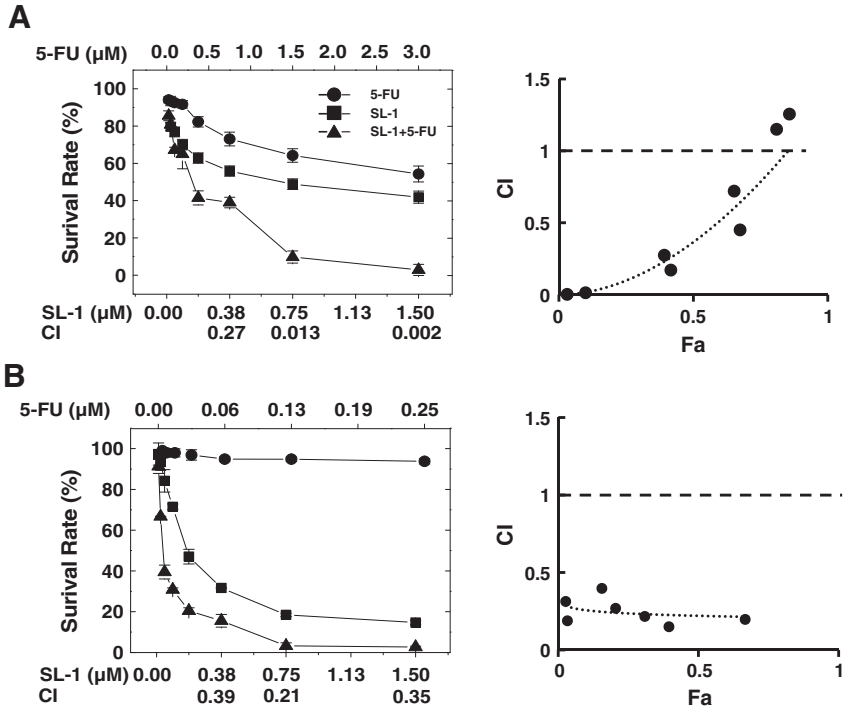

Figure 4. Synergistic suppression of the survival rate in (A) RKO and (B) SW620 cells co-treated with SL-1 and 5-FU. (A) RKO and (B) SW620 cells were treated with SL-1 and 5-FU alone or in combination at a ratio of 1:2 and 6:1, respectively. The survival rates (left) were analyzed by the PrestoBlue assay. The synergism or antagonism between different combined doses (right) was calculated using the combination index (CI), where CI = 1 indicates that the two drugs have additive effects, CI < 1 indicates better than additive effects ("synergism"), and CI > 1 indicates worse than additive effects ("antagonism").

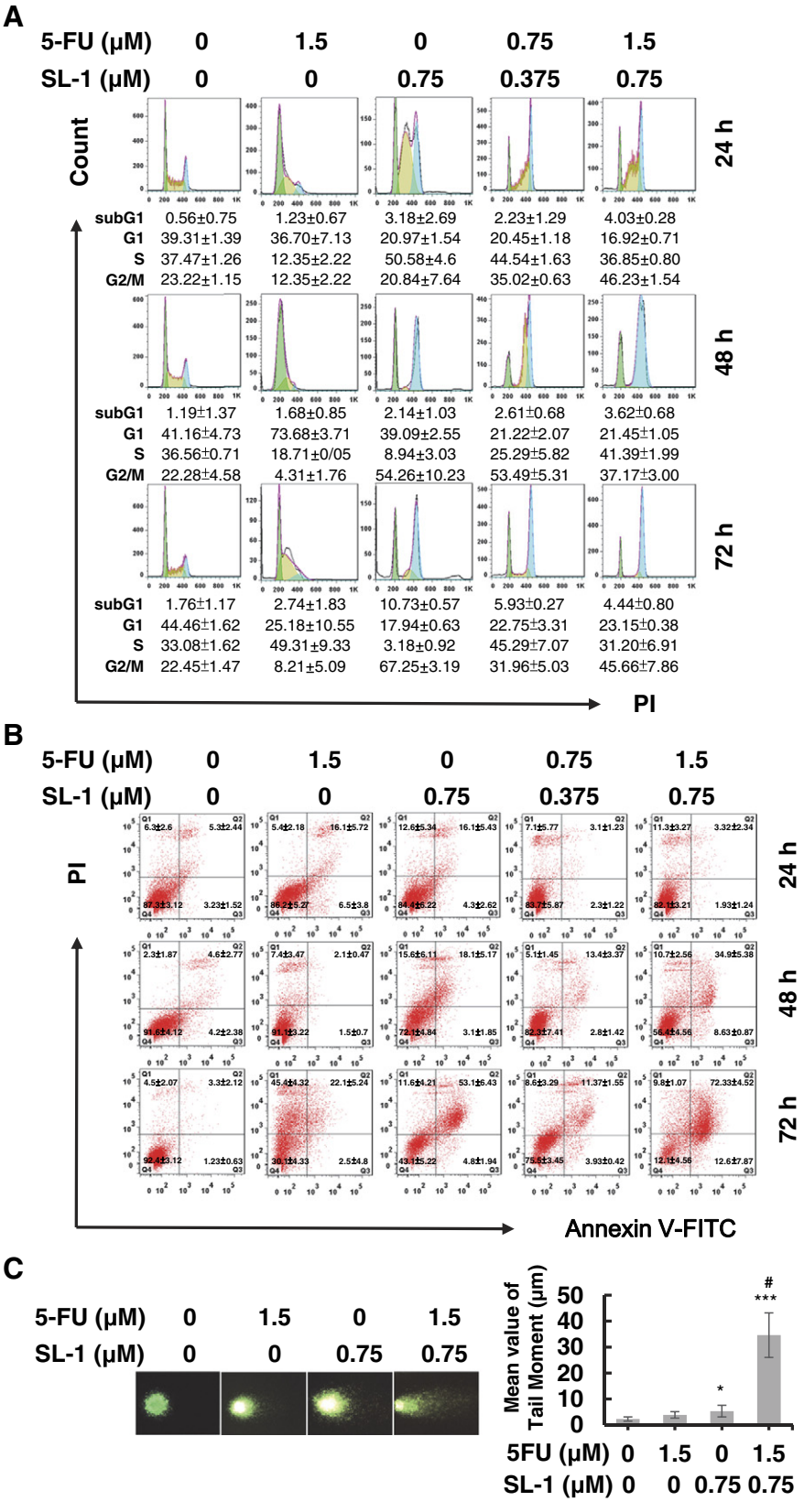

Figure 5. Enhanced G2/M arrest, apoptosis, and DNA damage by combination treatment of SL-1 and 5-FU. (A) Interference with cell cycle progression by combination treatment of SL-1 and 5-FU. RKO cells were treated with SL-1 and/or 5-FU for 24, 48, and 72 hours. Cell cycle analysis was performed using flow cytometry. (B) Enhanced apoptosis in RKO cells treated with SL-1 + 5-FU. After treatment of RKO cells with SL-1 and/or 5-FU at the indicated concentrations for 24, 48, or 72 hours, the cells were harvested and subjected to apoptosis analysis using annexin V-FITC and PI co-staining and flow cytometry. (C) Increased DNA strand breaks by combination treatment of SL-1 and 5-FU. RKO cells were treated with SL-1 and/or 5-FU for 24 hours and subjected to the comet assay. Left, representative tail moments; right, quantitative results expressed as the means ± SD ($n = 3$) (right). ***, $P < .001$; Student's t test. #, synergistic combination effect on increasing the tail moment, $CI_{comet\ assay} = 0.07$.

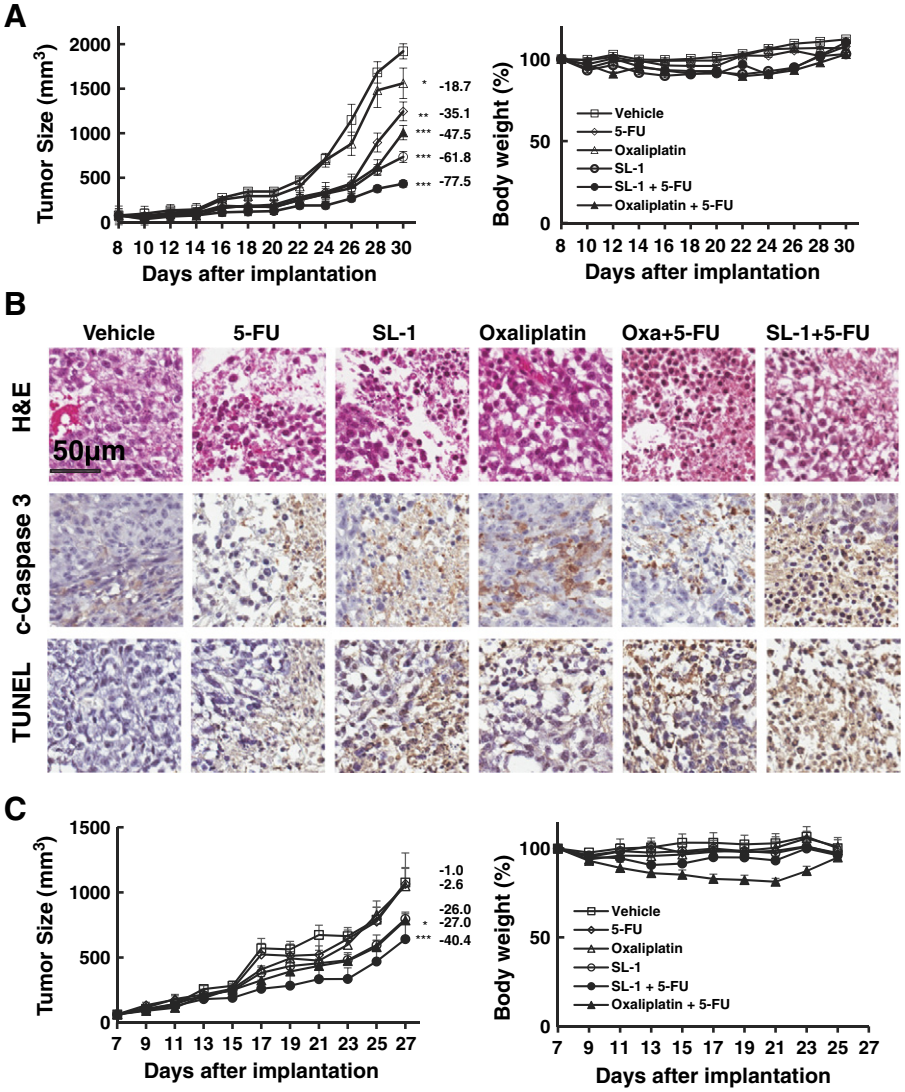

Figure 6. The therapeutic activity of SL-1 and combined with 5-FU on RKO and SW620 xenograft tumors. (A) Suppression of RKO xenografts by SL-1 and its combination with 5-FU. RKO (5×10^6) cells were subcutaneously implanted into nude mice. When the tumor size reached approximately 75 to 100 mm^3, the mice ($N = 5$ for each group) were treated with vehicles, SL-1, oxaliplatin, 5-FU, SL-1 + 5-FU, and oxaliplatin+ 5FU as described in Figure 3. SL-1 or oxaliplatin combined with 5-FU was administered using the same schedule. Left, tumor size; right, body weight change. (B) Increased apoptotic cell death in the RKO xenograft model. Xenograft tumors from one mouse from each group were sectioned 24 hours after the last treatment. The tumor sections were subjected to hematoxylin and eosin (H&E) staining, cleaved Caspase-3 immunochemical staining, and the TUNEL assay. (C) Suppression of SW620 xenografts by SL-1 and its combination with 5-FU. SW620 (5×10^6) were implanted, and the mice were treated as described in (A). Bar, S.E. ***, $P < .01$; Student's *t* test.

treatment of SL-1 + 5-FU was not as toxic as the combination of oxaliplatin and 5-FU.

SL-1 Displays Low Nephrotoxicity and Hepatotoxicity in Mice

To evaluate the toxicity of SL-1, ICR mice were treated with SL-1 (30 mg/kg), oxaliplatin (7.5 mg/kg), or cisplatin (7.5 mg/kg) alone or with combinations of SL-1 (30 mg/kg) + 5-FU (50 mg/kg) or oxaliplatin (7.5 mg/kg) + 5-FU (50 mg/kg). After 2 and 14 days of drug treatment, whole blood and serum were collected and subjected to complete blood count (CBC) and serum biochemistry analyses. The major organs were harvested for histopathology examination. As shown in Table 2, SL-1 did not cause significant changes in the results of the CBC analysis. However, we observed a slight increase in white blood cell counts (WBCs) in mice treated with cisplatin and oxaliplatin + 5-FU for 2 days. We also found that the red blood cell counts (RBCs) and platelet counts decreased in the groups receiving 5-FU, oxaliplatin, and oxaliplatin + 5-FU. In the serum biochemistry analysis, we noted that the levels of aspartate transaminase (AST) and alanine transaminase (ALT) significantly increased in mice treated with cisplatin, oxaliplatin, or oxliplatin + 5-FU but not in those treated with SL-1 or SL-1 + 5-FU, indicating that SL-1 displayed lower hepatotoxicity than cisplatin or oxaliplatin.

As expected, serum biochemical analysis revealed that the levels of blood urea nitrogen (BUN) and creatinine were increased in mice treated with cisplatin for 2 days (Table 2), confirming the nephrotoxicity of cisplatin. Nevertheless, there was no indication to show apparent kidney damage 2 days after treatment with SL-1 or

Table 2. Complete Blood Counts and Serum Biochemistry of ICR Mice Treated with SL-1 and Its Combinations for 2 Days[a,b,c,d]

Item	Unit	Vehicle	5-FU	SL-1	Oxaliplatin	Cisplatin	Oxa+ 5-FU	SL-1 + 5-FU
CBCs								
WBC	10^9/l	5.00 ± 0.74	5.09 ± 0.23	4.81 ± 1.00	5.76 ± 1.13	6.28 ± 1.10*	6.78 ± 0.98*	5.93 ± 0.54
NEUT	10^9/l	0.78 ± 0.30	0.78 ± 0.40	0.54 ± 0.20	0.52 ± 0.16	0.48 ± 0.26	0.50 ± 0.21	1.01 ± 0.75
LYMPH	10^9/l	4.07 ± 0.97	4.22 ± 0.45	3.55 ± 0.98	5.15 ± 1.12	5.54 ± 0.96*	5.88 ± 0.95*	4.80 ± 0.65
MONO	10^9/l	0.09 ± 0.05	0.02 ± 0.01	0.05 ± 0.03	0.03 ± 0.01*	0.04 ± 0.01	0.03 ± 0.01*	0.01 ± 0.01*
EO	10^9/l	0.13 ± 0.04	0.06 ± 0.01*	0.09 ± 0.03	0.04 ± 0.02**	0.09 ± 0.03	0.07 ± 0.03*	0.10 ± 0.03
BASO	10^9/l	0.03 ± 0.05	0.01 ± 0.01	0.00 ± 0.00	0.02 ± 0.02	0.02 ± 0.02	0.01 ± 0.01	0.01 ± 0.01
RBC	10^{12}/l	7.79 ± 1.16	4.98 ± 1.72*	7.80 ± 1.03	4.19 ± 2.66*	8.42 ± 1.49	4.38 ± 3.11*	7.28 ± 3.34
HGB	g/dl	13.30 ± 1.46	10.58 ± 2.62	12.34 ± 1.35	9.02 ± 5.40	13.63 ± 1.48	13.54 ± 1.51	13.72 ± 2.93
HCT	%	44.00 ± 3.49	27.94 ± 3.75***	38.32 ± 3.18	22.54 ± 13.33**	47.55 ± 1.77	25.16 ± 2.44**	42.60 ± 8.37
MCV	fl	52.88 ± 1.83	57.06 ± 3.75	58.18 ± 3.66	55.02 ± 2.64	54.40 ± 1.57	53.10 ± 2.76	55.10 ± 1.24
MCH	Pg	15.42 ± 0.37	14.94 ± 3.04	15.88 ± 0.48	22.08 ± 8.62	15.28 ± 2.52	16.02 ± 0.83	15.78 ± 2.58
MCHC	g/dl	29.16 ± 1.20	27.50 ± 4.71	25.86 ± 1.72	40.26 ± 15.97	26.48 ± 3.47	31.68 ± 3.03	26.37 ± 4.18
PLT	10^9/l	1463.60 ± 277.26	873.00 ± 141.40**	1742.40 ± 273.56	738.80 ± 347.09**	1095.50 ± 317.94*	385.20 ± 284.09***	785.20 ± 54.71**
Serum biochemistry								
AST	U/l	43.00 ± 8.25	63.50 ± 13.24*	49.00 ± 3.24	76.67 ± 16.47	70.00 ± 13.06**	81.00 ± 12.73**	50.25 ± 8.96
ALT	U/l	18.20 ± 4.71	23.25 ± 4.97	24.50 ± 2.17	28.00 ± 1.73	26.60 ± 7.70*	20.50 ± 4.95	24.00 ± 2.94
ALP	U/l	393.00 ± 98.54	359.25 ± 72.22	331.75 ± 27.94	498.33 ± 63.91	410.60 ± 82.16	362.00 ± 107.48	352.00 ± 76.25
GLU	mg/dl	178.40 ± 31.17	577.25 ± 36.55***	466.50 ± 146.80**	153.67 ± 88.22	183.40 ± 69.10	163.00 ± 19.80	357.75 ± 88.10**
BUN	mg/dl	22.84 ± 3.63	23.65 ± 1.50	23.05 ± 2.22	20.27 ± 3.32	30.68 ± 5.23**	26.00 ± 5.37	23.85 ± 2.61
CRE	mg/dl	0.14 ± 0.00	0.23 ± 0.1	0.20 ± 0.00	0.27 ± 0.06*	0.26 ± 0.09*	0.26 ± 0.20*	0.18 ± 0.05

[a] Male CD-1 (ICR) mice aged 5 weeks and with a body weight of 30 to 35 g were randomly allocated into seven groups (five mice/group): vehicle, 5-FU (50 mg/kg, i.p.); SL-1 (30 mg/kg, i.v.); oxaliplatin (7.5 mg/kg, i.v.); cisplatin (7.5 mg/kg, i.v.); Oxa+ 5-FU; SL-1 + 5-FU.

[b] Data are expressed as the mean ± SD (N = 4-5); *, $P < .05$; **, $P < .01$, ***, $P < .001$.

[c] WBC, white blood cells; NEU, neutrophils; LYM, lymphocytes; MONO, monocytes; EOS, eosinophils; BASO, basophils; RBC, red blood cells; HGB, hemoglobin; HCT, hematocrit; MCV, mean corpuscular volume; MCH, mean corpuscular hemoglobin; MCHC, mean corpuscular hemoglobin concentration; and PLT, platelet.

[d] AST, aspartate transaminase; ALT, alanine transaminase; ALP, alkaline phosphatase; BUN, blood urea nitrogen; CRE, creatinine; and GLU, glucose.

SL-1 + 5-FU. Notably, all damage was gradually recovered over the following 14 days (Table 3).

Furthermore, we did not observe obvious histologic damage in heart, spleen, and lung in any of the treatment groups (data not shown). Two days after SL-1 or SL-1 + 5-FU treatment, the renal lesions of the mice were tolerant to renal compensation, implying that the mice receiving single-dose treatment with SL-1 or SL-1 + 5-FU had insignificant morphological injury in the kidney (Figure 7). However, we found significant changes in the morphology of the renal medulla, such as distortion of the renal tube, nephron dilation, and bleeding with condensed nuclei in the partial medulla area in mice treated with cisplatin or oxaliplatin+ 5-FU (Figure 7), consistent with previous reports [29–31]. In a 14-day test, the renal injury was compensated in most of the groups, except the oxaliplatin+ 5-FU group. For liver toxicity, cisplatin treatment clearly displayed a moderate degree of fatty infiltrative change compared with oxaliplatin+ 5-FU in a 2-day test. The liver lesions in response to the oxaliplatin or SL-1 + 5-FU treatments shared a similar pattern but were less severe than those with cisplatin alone. While the liver damage was insignificant in mice treated with SL-1, the mild fatty change observed in the liver of mice treated with SL-1 + 5-FU might be due to 5-FU. In the 14-day test, most groups did not exhibit progression of toxicity in liver, as regeneration was observed. Importantly, histopathological examination showed that SL-1 by

Table 3. Complete Blood Counts and Serum Biochemistry of ICR Mice Treated with SL-1 and Its Combinations for 14 days[a]

Item[b]	Unit	Vehicle	5-FU	SL-1	Oxaliplatin	Cisplatin	Oxa+ 5-FU	SL-1 + 5-FU
CBCs								
WBC	10^9/l	5.67 ± 1.46	3.40 ± 1.21	5.50 ± 1.64	2.78 ± 0.98**	6.02 ± 1.96	3.45 ± 0.79	3.88 ± 0.35
NEUT	10^9/l	0.79 ± 0.26	0.64 ± 0.17	1.08 ± 0.36	0.52 ± 0.14	1.47 ± 0.97	0.88 ± 0.23	1.06 ± 0.41
LYMPH	10^9/l	4.56 ± 1.37	2.62 ± 0.94	4.17 ± 1.28	2.14 ± 0.83*	4.32 ± 1.04	2.91 ± 0.63	2.55 ± 0.26*
MONO	10^9/l	0.16 ± 0.04	0.06 ± 0.10	0.12 ± 0.15	0.06 ± 0.09	0.10 ± 0.09	0.10 ± 0.08	0.13 ± 0.05
EO	10^9/l	0.16 ± 0.01	0.08 ± 0.01***	0.13 ± 0.05	0.06 ± 0.02***	0.12 ± 0.03	0.07 ± 0.06*	0.14 ± 0.02
BASO	10^9/l	0.01 ± 0.01	0.01 ± 0.01	0.01 ± 0.01	0.01 ± 0.01	0.00 ± 0.01	0.01 ± 0.01	0.01 ± 0.01
RBC	10^{12}/l	9.18 ± 0.19	8.06 ± 0.24***	8.60 ± 0.68	8.05 ± 0.41**	8.74 ± 0.79	8.54 ± 0.55	8.74 ± 0.32*
HGB	g/dl	14.25 ± 0.37	13.08 ± 0.25**	13.36 ± 0.74	13.12 ± 0.73*	13.46 ± 1.24	13.69 ± 0.76	12.82 ± 0.13
HCT	%	48.60 ± 0.85	45.53 ± 1.61*	46.28 ± 2.32	43.32 ± 2.86*	45.54 ± 4.58	46.37 ± 2.35	48.83 ± 0.32
MCV	fl	52.95 ± 1.21	56.48 ± 1.73*	53.96 ± 1.92	53.78 ± 1.04	52.14 ± 2.48	54.34 ± 0.89	55.47 ± 2.29
MCH	Pg	15.53 ± 0.46	16.25 ± 0.35*	15.58 ± 0.47	16.30 ± 0.43*	15.42 ± 0.40	16.04 ± 0.24*	16.13 ± 0.40
MCHC	g/dl	29.30 ± 0.26	28.73 ± 0.48	28.84 ± 0.57	30.28 ± 0.75*	29.60 ± 0.76	29.50 ± 0.42	29.13 ± 0.55
PLT	10^9/l	953.25 ± 57.12	745.75 ± 116.31*	838.80 ± 57.98	692.20 ± 192.91*	772.20 ± 349.78	732.71 ± 289.62	1006.67 ± 17.01
Serum biochemistry								
GOT/AST	U/l	48.50 ± 4.43	53.00 ± 3.56	47.50 ± 1.29	47.25 ± 7.13	46.5 ± 2.12	66.2 ± 3.63***	56.40 ± 5.68*
GPT/ALT	U/l	29.50 ± 5.46	46.50 ± 7.85	22.00 ± 8.04	29.50 ± 5.74	37.50 ± 6.36	33.80 ± 7.92	34.00 ± 9.41
ALP	U/l	341.75 ± 72.77	177.50 ± 119.69*	231.00 ± 85.33*	245.5 ± 35.07	282.50 ± 19.09	206.00 ± 81.09*	306.40 ± 188.06
GLU	mg/dl	229.75 ± 69.82	244.00 ± 86.63	219.75 ± 35.85	268.25 ± 61.43	285.50 ± 65.76	301.60 ± 89.49	259.60 ± 102.12
BUN	mg/dl	19.20 ± 2.59	22.20 ± 3.42	20.05 ± 2.37	21.35 ± 5.07	22.70 ± 1.56	26.66 ± 6.03	23.72 ± 3.77
CRE	mg/dl	0.10 ± 0.00	0.25 ± 0.10*	0.17 ± 0.06	0.13 ± 0.05	0.15 ± 0.07	0.20 ± 0.07*	0.14 ± 0.05

[a] Experimental protocol and all symbols are the same as in Table 2.

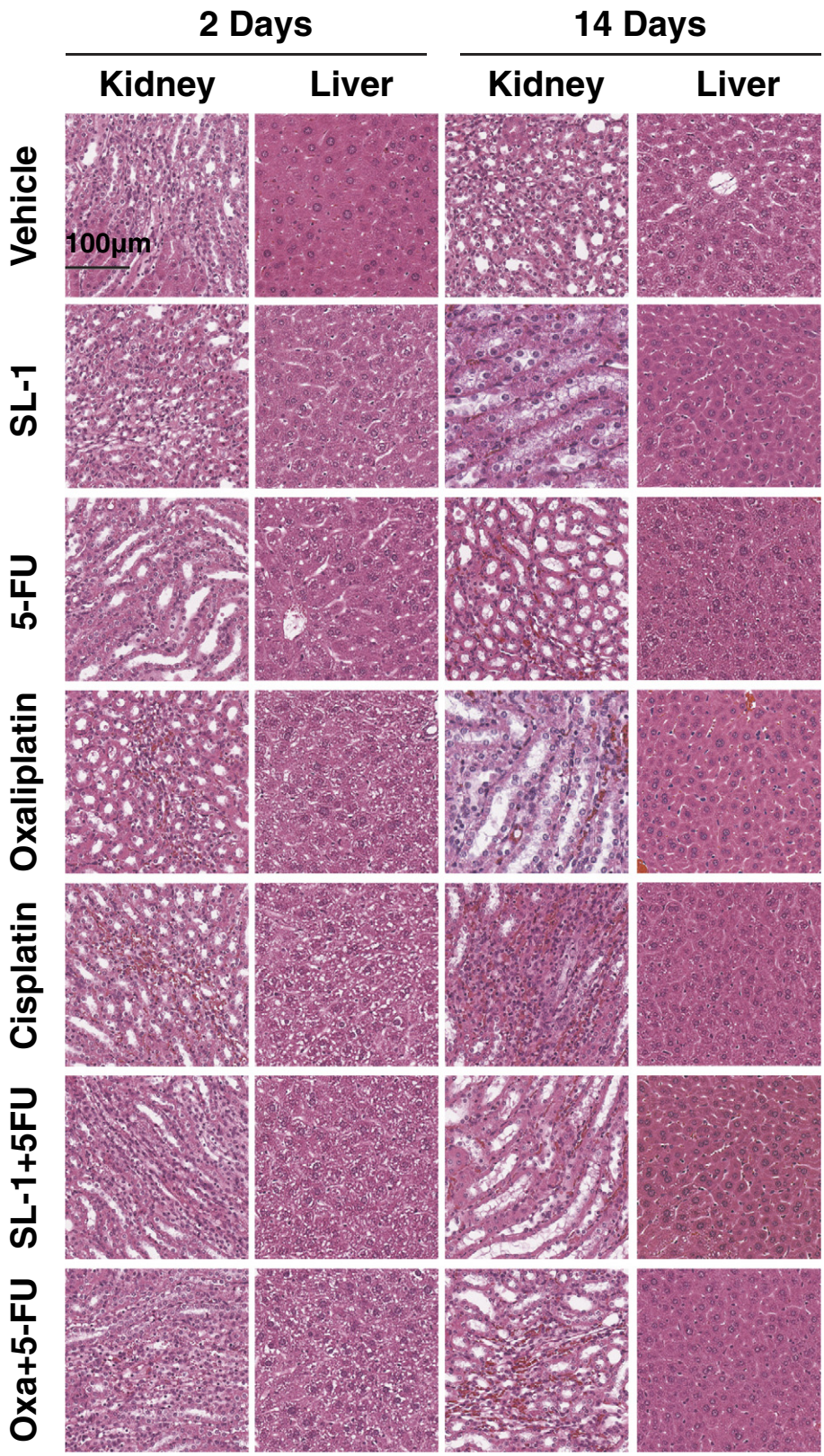

Figure 7. Histopathological examination of kidney and liver in ICR mice treated with various drug combinations. The kidney and liver from ICR mice treated with one shot of SL-1 (30 mg/kg, i.v.), 5-FU (50 mg/kg, i.p.), oxaliplatin (7.5 mg/kg, i.v.), or the combination of SL-1 + 5-FU or oxaliplatin + 5-FU were subjected to histopathological examination at 2 or 14 days after treatment. Tissue sections were stained with H&E and examined under a microscope.

itself caused no obvious nephrotoxicity or hepatotoxicity in ICR mice compared with cisplatin, oxaliplatin, or 5-FU.

Discussion

While DNA-alkylating agents are used widely as first-line drugs for various cancers, the main limitations of simple alkylating agents are their lack of DNA sequence specificity [32]. Melphalan mainly induces dG-adducts at 5′-GNC-3′ and 5′-GC-3′ base pairs [32], whereas the platinum-based drugs principally bind to 5′-GG-3′ and 5′-GC-3′ base pairs [33]. In addition, the platinum-based alkylating agents generate more monoalkylation products than cross-links [33–35]. This observation may explain why platinum-based alkylating agents not only cause increased mutagenesis and carcinogenesis but also induce adverse side effects. To overcome these drawbacks, a DNA-directed alkylating agent with increased DNA-binding selectivity and reduced cytotoxicity was proposed [36].

In this study, we demonstrated that *N*-mustard-quinoline conjugates such as SL-1 and SL-2 preferentially targeted certain dG residues with the consensus sequence 5′-G-G/C-N-G-C/T-3′. This unique binding preference was not observed in the other *N*-mustard derivatives linked to different DNA-affinic carriers (such as acridine, 9-alinioacridines, or quinazolines) synthesized in our laboratory. As shown in Supplementary Figure S4 and S5, no distinct binding sequence was observed with an *N*-mustard 9-anilinoacridine conjugate (BO-1051) [6] and unmasked water soluble *N*-benzene mustard conjugates (BO-1055) [8]. These results suggested that the quinoline pharmacophore plays an important role in drug efficacy and safety.

Intriguingly, McClean et al. [37] reported that when interacting with DNA, quaternary *N*-mustard 4-anilinoquinolinium conjugates (Supplementary Figure S7) bind strongly to AT-rich sequences in the minor groove. It remains unclear why the 6,7-methylenedioxy-quinoline pharmacophore in SL-1 prefers laying on 5′-G-C/T-3′, whereas the quaternary *N*-mustard 4-anilinoquinolinium conjugates favor binding to AT-rich minor grooves *via* their methyl quaternary salt. Since the linkers used in the SL-1 and the *N*-mustard-4-anilinoquinoline conjugate are hydrazinecarboxamide and aniline, respectively, we could not rule out the possibility that different linkers might induce varied sequence preferences before anchoring alkylation. However, unlike cisplatin and unmasked *N*-mustard conjugates, SL-1 creates sequence-dependent guanine adducts, which may reduce the inevitable side effects.

We have compared the potency of a series of DNA-directed alkylating agents, including *N*-mustard-acridine, *N*-mustard-quinoline, and *N*-mustard-quinazoline conjugates previously synthesized in our laboratory [7,13], and currently used drugs (oxaliplatin, cisplatin, or 5-FU) for the treatment of CRC patients. Among these compounds, we found that SL-1 was the most effective. Notably, we found that p53-dependent RKO cells and metastatic p53-MT SW620 cell lines were sensitive to SL-1, indicating that SL-1 may serve as a useful agent against p53-MT CRC cells. Additionally, SL-1 also effectively killed p53-independent RKO-E6 cells, which were resistant to cisplatin. In addition, SL-1 was more potent than cisplatin in causing DNA strand breaks and ICLs and in triggering apoptotic cell death. For the drug safety study, we found that SL-1 displayed low toxicity to normal colon epithelial FHC cells, indicating that SL-1 has a wider therapeutic window than the therapeutic agents used clinically (e.g., oxaliplatin, cisplatin, 5-FU, and irinotecan). These results strongly suggest that SL-1 targets to a wide spectrum of CRC cell lines, including mCRC cells.

We demonstrated that SL-1 alone exhibited more tumor suppression in nude mice bearing RKO (p53-dependent) or RKO-E6 (p53-independent) xenografts than 5-FU, cisplatin, or oxaliplatin. This result suggests that SL-1 may act as an agent against CRC cells that are resistant to oxaliplatin. Although FOLFOX resulted in significantly increased response rates and improved survival, the combination treatment with oxaliplatin and 5-FU still manifested an increase in the side effects of these two drugs, such as bone marrow suppression, gastrointestinal toxicity, delayed neurotoxicity, and, less frequently, congestive heart failure [38]. Therefore, a new strategy for the treatment of CRC patients with combination therapy that would minimize the unpleasant side effects is urgently needed. In the present study, we showed that 5-FU synergistically increased the cytotoxicity of SL-1 against various p53-WT and p53-MT CRC cell lines *in vitro*. Furthermore, the combination of SL-1 + 5-FU synergistically triggered apoptotic cell death and increased the tail moment by damaging DNA. In addition, we found that the antitumor effects of the combination of 5-FU and SL-1 were more potent than those of oxaliplatin + 5-FU in mice bearing RKO (p53-WT) and metastatic SW620 (p53-MT) xenografts. Accordingly, the combination of SL-1 + 5-FU is a potential regimen for the treatment of patients with CRC.

Most alkylating agents have good therapeutic efficacy in cancer cells but are toxic to normal cells. Based on the design principles of DNA-directed alkylating agents, SL-1 might alleviate side effects in comparison to other alkylating agents because the DNA sequence preference of SL-1 may reduce its toxicity to animals. We evaluated the toxicity of SL-1 by intravenously injecting the compound into ICR mice. We did not observe obvious damage to the major organs or blood biochemistry changes in the SL-1–treated mice. Conversely, we observed that 5-FU, cisplatin, and oxaliplatin induced some toxicity, such as cytopenia, nephrotoxicity, and liver toxicity, respectively. We also confirmed the kidney damage caused by cisplatin and the spectrum of changes in focal vascular injury and cellular swelling. Moreover, cisplatin treatment increased the BUN value by 30% after 2 days. Additionally, the platelet and neutrophil counts were decreased by oxaliplatin, as reported previously [29,31]. These results indicated that SL-1 at the tested dose has a better safety profile in animals than the other tested control compounds. SL-1 was the first designed DNA-directed alkylating agent shown to be less toxic *in vivo*. However, whether the selective alkylation by SL-1 is a reason for reduced adverse side effects warrants further investigation.

In summary, the quinoline moiety in SL-1, which functions as a DNA-affinic carrier, may play a key role in defining the DNA-binding geometry and maintaining the potential region and sequence specificity of the alkylation. SL-1 alone or in combination with 5-FU displayed potent antitumor efficacy in nude mice bearing RKO (p53-WT) and metastatic SW620 (p53-MT) xenografts, suggesting that this agent may be effective for the treatment of patients with mCRC. Remarkably, compared with other antitumor agents, SL-1 and SL-1 + 5-FU displayed a better safety profile. Accordingly, SL-1 has great potential for development as an anticancer agent for the treatment of CRC patients.

Acknowledgements

We thank Dr. Tai-Yuan Yu and Miss Chun-Ping Chang for helping with the drug/DNA sequence specificity study. We also thank the Chemical Synthesis Core and the Pathology Core Laboratory of IBMS for synthesizing SL-1 and for performing the pathology

analysis, respectively, and the Taiwan Mouse Clinic (MOST 105-2325-B-001-010), which is funded by the National Research Program for Biopharmaceuticals at the Ministry of Science and Technology of Taiwan, for technical support with the blood cells and blood biochemistry analysis. The mass spectrometry analysis was supported by the Metabolomics Core Facility, Scientific Instrument Center at Academia Sinica. This work was supported in part by grants from the Ministry of Science and Technology, Taiwan (MOST103-2325-B-001-018, MOST104-2325-B-001-001, and MOST 105-2325-B-001-001), and Academia Sinica (AS-102-TP-B13) to T. C. L. and by a grant from the Ministry of Science and Technology (MOST 105-0210-01-13-01) and an intramural grant from Academia Sinica to C. N. S.

Appendix A. Supplementary data

Supplementary data to this article can be found online at https://doi.org/10.1016/j.neo.2017.11.006.

References

[1] Goodman LS and Wintrobe MM, et al (1946). Nitrogen mustard therapy; use of methyl-bis (beta-chloroethyl) amine hydrochloride and tris (beta-chloroethyl) amine hydrochloride for Hodgkin's disease, lymphosarcoma, leukemia and certain allied and miscellaneous disorders. *JAMA* **132**, 126–132.

[2] Shewach DS and Kuchta RD (2009). Introduction to cancer chemotherapeutics. *Chem Rev* **109**, 2859–2861.

[3] Brendel M and Ruhland A (1984). Relationships between functionality and genetic toxicology of selected DNA-damaging agents. *Mutat Res* **133**, 51–85.

[4] Gravatt GL, Baguley BC, Wilson WR, and Denny WA (1991). DNA-directed alkylating agents. 4. 4-anilinoquinoline-based minor groove directed aniline mustards. *J Med Chem* **34**, 1552–1560.

[5] Bacherikov VA, Chou TC, Dong HJ, Zhang X, Chen CH, Lin YW, Tsai TJ, Lee RZ, Liu LF, and Su TL (2005). Potent antitumor 9-anilinoacridines bearing an alkylating N-mustard residue on the anilino ring: synthesis and biological activity. *Bioorg Med Chem* **13**, 3993–4006.

[6] Kapuriya N, Kapuriya K, Zhang X, Chou TC, Kakadiya R, Wu YT, Tsai TH, Chen YT, Lee TC, and Shah A, et al (2008). Synthesis and biological activity of stable and potent antitumor agents, aniline nitrogen mustards linked to 9-anilinoacridines via a urea linkage. *Bioorg Med Chem* **16**, 5413–5423.

[7] Kapuriya N, Kapuriya K, Dong H, Zhang X, Chou TC, Chen YT, Lee TC, Lee WC, Tsai TH, and Naliapara Y, et al (2009). Novel DNA-directed alkylating agents: design, synthesis and potent antitumor effect of phenyl N-mustard-9-anilinoacridine conjugates via a carbamate or carbonate linker. *Bioorg Med Chem* **17**, 1264–1275.

[8] Kapuriya N, Kakadiya R, Dong H, Kumar A, Lee PC, Zhang X, Chou TC, Lee TC, Chen CH, and Lam K, et al (2011). Design, synthesis, and biological evaluation of novel water-soluble N-mustards as potential anticancer agents. *Bioorg Med Chem* **19**, 471–485.

[9] Denny WA (2001). DNA minor groove alkylating agents. *Curr Med Chem* **8**, 533–544.

[10] Gourdie TA, Valu KK, Gravatt GL, Boritzki TJ, Baguley BC, Wakelin LP, Wilson WR, Woodgate PD, and Denny WA (1990). DNA-directed alkylating agents. 1. Structure-activity relationships for acridine-linked aniline mustards: consequences of varying the reactivity of the mustard. *J Med Chem* **33**, 1177–1186.

[11] Shinohara K, Bando T, Sasaki S, Sakakibara Y, Minoshima M, and Sugiyama H (2006). Antitumor activity of sequence-specific alkylating agents: pyrolle-imidazole CBI conjugates with indole linker. *Cancer Sci* **97**, 219–225.

[12] Hurley LH (2002). DNA and its associated processes as targets for cancer therapy. *Nat Rev Cancer* **2**, 188–200.

[13] Kakadiya R, Dong H, Kumar A, Narsinh D, Zhang X, Chou TC, Lee TC, Shah A, and Su TL (2010). Potent DNA-directed alkylating agents: synthesis and biological activity of phenyl N-mustard-quinoline conjugates having a urea or hydrazinecarboxamide linker. *Bioorg Med Chem* **18**, 2285–2299.

[14] Field K and Lipton L (2007). Metastatic colorectal cancer—past, progress and future. *World J Gastroenterol* **13**, 3806–3815.

[15] Alcindor T and Beauger N (2011). Oxaliplatin: a review in the era of molecularly targeted therapy. *Curr Oncol* **18**, 18–25.

[16] Tournigand C, Cervantes A, Figer A, Lledo G, Flesch M, Buyse M, Mineur L, Carola E, Etienne PL, and Rivera F, et al (2006). OPTIMOX1: a randomized study of FOLFOX4 or FOLFOX7 with oxaliplatin in a stop-and-go fashion in advanced colorectal cancer–a GERCOR study. *J Clin Oncol* **24**, 394–400.

[17] Andre T, Boni C, Mounedji-Boudiaf L, Navarro M, Tabernero J, Hickish T, Topham C, Zaninelli M, Clingan P, and Bridgewater J, et al (2004). Oxaliplatin, fluorouracil, and leucovorin as adjuvant treatment for colon cancer. *N Engl J Med* **350**, 2343–2351.

[18] Siegel RL, Miller KD, and Jemal A (2016). Cancer statistics, 2016. *CA Cancer J Clin* **66**, 7–30.

[19] El-Shami K, Oeffinger KC, Erb NL, Willis A, Bretsch JK, Pratt-Chapman ML, Cannady RS, Wong SL, Rose J, and Barbour AL, et al (2015). American Cancer Society colorectal cancer survivorship care guidelines. *CA Cancer J Clin* **65**, 428–455.

[20] Hampshire AJ and Fox KR (2008). Preferred binding sites for the bifunctional intercalator TANDEM determined using DNA fragments that contain every symmetrical hexanucleotide sequence. *Anal Biochem* **374**, 298–303.

[21] Hampshire AJ and Fox KR (2008). The effects of local DNA sequence on the interaction of ligands with their preferred binding sites. *Biochimie* **90**, 988–998.

[22] Hampshire AJ, Rusling DA, Broughton-Head VJ, and Fox KR (2007). Footprinting: a method for determining the sequence selectivity, affinity and kinetics of DNA-binding ligands. *Methods* **42**, 128–140.

[23] Anderson JW, Fox KR, and Niblo GA (2006). A fast algorithm for the construction of universal footprinting templates in DNA. *J Math Biol* **52**, 307–342.

[24] Chen CW, Wu MH, Chen YF, Yen TY, Lin YW, Chao SH, Tala S, Tsai TH, Su TL, and Lee TC (2016). A potent derivative of indolizino[6,7-b]indole for treatment of human non–small cell lung cancer cells. *Neoplasia* **18**, 199–212.

[25] Lee PC, Kakadiya R, Su TL, and Lee TC (2010). Combination of bifunctional alkylating agent and arsenic trioxide synergistically suppresses the growth of drug-resistant tumor cells. *Neoplasia* **12**, 376–387.

[26] Crooks GE, Hon G, Chandonia JM, and Brenner SE (2004). WebLogo: a sequence logo generator. *Genome Res* **14**, 1188–1190.

[27] *Efficacy of adjuvant fluorouracil and folinic acid in colon cancer. International Multicentre Pooled Analysis of Colon Cancer Trials (IMPACT) investigatorsLancet* **345**, 939–944.

[28] Longley DB, Harkin DP, and Johnston PG (2003). 5-fluorouracil: mechanisms of action and clinical strategies. *Nat Rev Cancer* **3**, 330–338.

[29] Hanada K, Suda M, Kanai N, and Ogata H (2010). Pharmacokinetics and toxicodynamics of oxaliplatin in rats: application of a toxicity factor to explain differences in the nephrotoxicity and myelosuppression induced by oxaliplatin and the other platinum antitumor derivatives. *Pharm Res* **27**, 1893–1899.

[30] Mathe G, Kidani Y, Noji M, Maral R, Bourut C, and Chenu E (1985). Antitumor activity of l-OHP in mice. *Cancer Lett* **27**, 135–143.

[31] Dobyan DC, Levi J, Jacobs C, Kosek J, and Weiner MW (1980). Mechanism of cis-platinum nephrotoxicity: II. Morphologic observations. *J Pharmacol Exp Ther* **213**, 551–556.

[32] Mattes WB, Hartley JA, and Kohn KW (1986). DNA-sequence selectivity of guanine-N7 alkylation by nitrogen mustards. *Nucleic Acids Res* **14**, 2971–2987.

[33] Jamieson ER and Lippard SJ (1999). Structure, recognition, and processing of cisplatin-DNA adducts. *Chem Rev* **99**, 2467–2498.

[34] Kohn KW, Hartley JA, and Mattes WB (1987). Mechanisms of DNA sequence selective alkylation of guanine-N7 positions by nitrogen mustards. *Nucleic Acids Res* **15**, 10531–10549.

[35] Kelland L (2007). The resurgence of platinum-based cancer chemotherapy. *Nat Rev Cancer* **7**, 573–584.

[36] Wyatt MD, Lee M, Garbiras BJ, Souhami RL, and Hartley JA (1995). Sequence specificity of alkylation for a series of nitrogen mustard-containing analogues of distamycin of increasing binding site size: evidence for increased cytotoxicity with enhanced sequence specificity. *Biochemistry* **34**, 13034–13041.

[37] McClean S, Costelloe C, Denny WA, Searcey M, and Wakelin LP (1999). Sequence selectivity, cross-linking efficiency and cytotoxicity of DNA-targeted 4-anilinoquinoline aniline mustards. *Anticancer Drug Des* **14**, 187–204.

[38] Stojanovska V, Sakkal S, and Nurgali K (2015). Platinum-based chemotherapy: gastrointestinal immunomodulation and enteric nervous system toxicity. *Am J Physiol Gastrointest Liver Physiol* **308**, G223–232.